



Universiteit
Leiden
The Netherlands

Spin-label EPR Approaches to Protein Interactions

Son, M. van

Citation

Son, M. van. (2014, December 4). *Spin-label EPR Approaches to Protein Interactions*. *Casimir PhD Series*. Retrieved from <https://hdl.handle.net/1887/29986>

Version: Not Applicable (or Unknown)

License: [Leiden University Non-exclusive license](#)

Downloaded from: <https://hdl.handle.net/1887/29986>

Note: To cite this publication please use the final published version (if applicable).

Cover Page



Universiteit Leiden



The handle <http://hdl.handle.net/1887/29986> holds various files of this Leiden University dissertation.

Author: Son, Martin van

Title: Spin-label EPR approaches to protein interactions

Issue Date: 2014-12-04

5

EQUILIBRIUM UNFOLDING OF FLAVODOXIN FROM DOUBLE ELECTRON-ELECTRON RESONANCE DISTANCE CONSTRAINTS

5.1 Introduction

Protein folding is one of the most fascinating aspects of protein biochemistry. Insight into the process requires structural information on the protein chain at different folding states. Novel methods are sought to obtain experimental data on the folding process. Electron-paramagnetic-resonance techniques are well suited to follow the folding process, because they can determine distances and dynamics. Several EPR studies targeting folding of proteins have been reported, either based on steady-state^[1;2] or flow methods^[3-7].

Here we describe double electron-electron spin resonance (DEER) experiments performed under equilibrium unfolding conditions. The goal is to directly monitor *local* structure of the protein during unfolding by monitoring the distance between spin labels. Previous studies employing EPR were focused on local mobility changes, for example^[1;3], or distance measurements by EPR-line broadening^[4].

The present study describes the unfolding of holo-flavodoxin with guanidine hydrochloride (GuHCl)^[8] as unfolding agent. Flavodoxin folding has been the subject of several studies^[8-14]. The native-state structure of holo-flavodoxin is shown in Figure 5.1. Site-directed, spin-label mutagenesis was

performed to replace the native residue at position 131 by a cysteine. The native cysteine at position 69 serves as the second site for spin labelling with the nitroxide spin label MTSL. In the following we refer to the spin-labelled protein as fdx-SL. By DEER, we measure the distance between the two spin-label nitroxide groups. We interpret the distance in the native state, i.e., in the absence of GuHCl and the development of the distance distribution as a function of GuHCl concentration.

We demonstrate that we can follow the unfolding by DEER and detect changes in local structure upon unfolding. The distance distributions reveal the presence of proteins in conformations that are different from the native state and have well defined structure, indicative of folding intermediates.

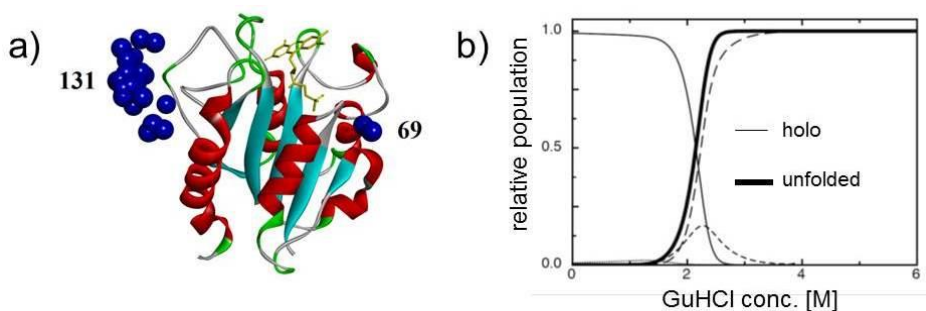


Figure 5.1 The structure of flavodoxin (fdx) based on the crystal structure (PDB entry 1YOB) with the flavine cofactor (in yellow). The blue spheres show representative locations of the nitroxide of the spin label, which is attached at positions 69 and 131 in the protein, as derived from the MMM simulation of protein A in the crystallographic unit cell. b) Normalized equilibrium population of holo-fdx (thin solid line), native apo-fdx (dots), off-pathway molten globule (short dashes) and unfolded protein (long dashes) as determined in reference [9]. The thick solid line represents the fraction of non-native molecules (i.e., the sum of off-pathway intermediate and unfolded protein).

5.2 Material and methods

Purification and spin labelling of flavodoxin D131C

The apo-fdx mutant D131C was generated and purified as described elsewhere^[8]. This variant contains the wild-type cysteine residue at position 69 as well as a cysteine residue at position 131. Prior to labelling of the protein with spin-label MTSL (Toronto Research Chemicals), the protein was unfolded in 5 M GuHCl, and incubated with dithiothreitol DTT to reduce the thiol-groups of the cysteines. The reductant DTT was removed by gel filtration with a P6-DG column (Bio-Rad), which was equilibrated with 5 M GuHCl (Fluka) in 50mM potassium phosphate (Sigma-Aldrich) buffer at pH 7.5. Labelling with MTSL was carried out during 16 hours at 4 °C, using a 20-fold molar excess of spin label over protein. The resulting doubly spin-labelled protein was purified from excess spin label and GuHCl by gel filtration on a Superdex 75 10/30 HR column (Pharmacia), which was equilibrated in 100 mM potassium pyrophosphate (Sigma-Aldrich) at pH 6.0. The apo-fdx thus obtained was incubated with an excess of flavin mononucleotide (FMN) to reconstitute the holoprotein. Free FMN was separated from holo-fdx by gel filtration on a Superdex 75 10/30 HR column.

The purification and spin labelling of flavodoxin was done by Simon Lindhoud (Laboratory of Biochemistry at Wageningen University and Research Centre).

Sample preparation

Guanidine hydrochloride (GuHCl) was used as a denaturant for the folding study. Due to the hygroscopy of GuHCl, it was not possible to use conventional means to prepare solutions with this compound in accurate concentrations.

Instead, we made a stock solution with an accurate concentration of GuHCl by measuring the refractive index of this solution and by using the relation

$$Z = 57.147\Delta N + 38.68(\Delta N)^2 - 91.60(\Delta N)^3, \quad (5.1)$$

where Z is the concentration of GuHCl in M and ΔN is the difference between the refractive indices of the buffer solution with and without GuHCl^[15]. The final concentrations of GuHCl used in the DEER measurements are mentioned in Table 5.1.

In each of the measurements, the protein concentration was about 0.1 mM. The buffer was 100 mM potassium pyrophosphate (KPP_i), pH 6.0, with 20% glycerol. The protein solutions were placed in quartz tubes with an id/od of 2.3 mm/3.0 mm. The samples that contained GuHCl were incubated at room temperature and in the dark for 12 hours.

A quantitative analysis of the spin-label concentration was made by double integration of the 80 K cw-EPR spectrum and comparison to the spectrum of MTSL with known spin concentration. Based on this analysis, we found that at least 83% of the fdx cysteines were spin labelled. The cw-EPR spectrum of a doubly labelled species is expected to show line broadening compared to the spectrum of a monoradical reference, when measured under the same conditions, if the spin labels are separated by less than 2 nm^[16].

Continuous wave EPR-measurements

The cw-EPR measurements were performed at 9.8 GHz using an ELEXSYS E 680 spectrometer (Bruker BioSpin GmbH, Rheinstetten, Germany) equipped with a rectangular cavity and a cryostat. A flow of liquid helium was directed through the cavity to maintain a temperature of 80 K. The spectra were recorded at a microwave power of 0.16 mW with a field sweep of 20 mT and

2048 field points. Field modulation at a frequency of 100 kHz was employed with an amplitude of 0.2 mT. The time constant was 41 ms with a conversion time of 41 ms. The measurement time was 15 to 30 minutes per sample.

DEER measurements and data analysis

The four-pulse DEER experiments were performed at 9.3 GHz using an ELEXSYS E 680 spectrometer (Bruker BioSpin GmbH, Rheinstetten, Germany) equipped with a split-ring cavity and a cryostat, Oxford model CF 935. A flow of liquid helium was directed through the cavity to maintain a temperature of 40 K. The DEER sequence is described in section 1.4. The separation between the frequencies was about 65 MHz. The observer pulses had lengths of 16 and 32 ns, the pump pulse had a length of 16 ns. The delay times were $\tau_1 = 140$ ns and $\tau_2 = 3.6$ μ s. The total time of a DEER measurement was about 15 hours.

Each of the DEER measurements was directly followed by a reference measurement. The sample for these reference measurements was a solution of a rigid biphenyl bi-radical in methyl tetrahydrofuran, contained in a quartz tube with an id/od of 2.3 mm/3.0 mm. Oxygen had been removed from the solution by four repeated freeze-thaw cycles, followed by flame sealing to close the tube.

The DEER data was analysed and fit with the DeerAnalysis2011 program^[17]. We assumed a homogenous three-dimensional background. The validation option within the software was used to find a consistent background start, resulting in 600 ns for the protein solutions with low denaturant concentrations (0, 0.3 M, 0.8 M, and 2.3 M) and 1720 ns for the high concentrations (3.5 M and 4.5 M).

5.3 Results

We study the unfolding of the doubly spin-labelled fdx mutant 131C (fdx-SL), which contains a native cysteine at position 69 and an engineered cysteine at position 131. The protein used is 85% spin labelled (see Materials and methods) and the sample did not contain free spin label, as determined by cw EPR experiments at room temperature (data not shown).

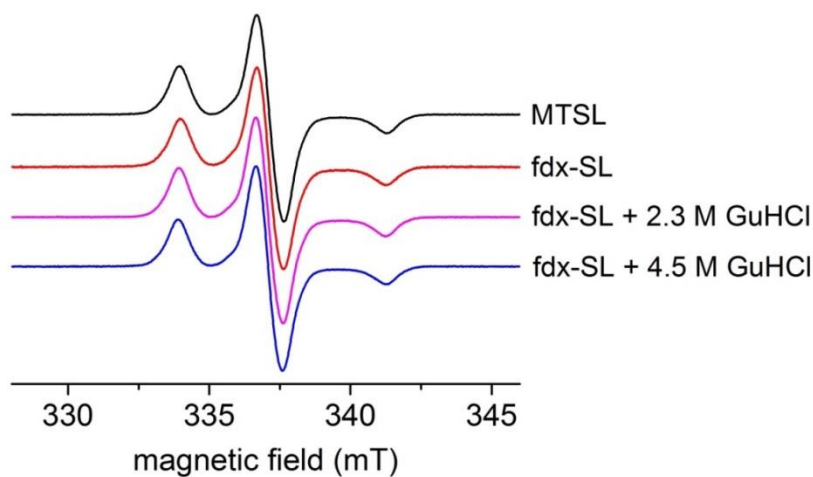


Figure 5.2 The cw-EPR spectra recorded at 80 K of MTSL (black), native fdx-SL (red), fdx-SL + 2.3 M GuHCl (pink), and fdx-SL + 4.5 M GuHCl (blue). The spectra are shifted vertically for better viewing.

The results of frozen solution cw EPR are shown in Figure 5.2. Regarding the lineshape, the cw-EPR spectra of the protein in frozen solution are identical to the spectra of a monomeric reference, thus no line broadening was detected. In Figure 5.3, all DEER-time traces are collected. Figure 5.3a shows the raw time traces and the background, and Figure 5.3b the background corrected traces. First, we will describe the results obtained on fdx-SL in the native state, i.e., in

the absence of GuHCl, and then we will describe the results of the series of DEER experiments performed on fdx-SL at different GuHCl concentrations.

The DEER-time trace of fdx-SL in the absence of GuHCl, shown in Figure 5.3a, has an initial decay and hardly any structure, i.e., visible modulation. The modulation depth corresponds to that expected for two coupled spins, which shows that the entire protein population contributes to the distance distribution shown in Figure 5.4. The distribution has two peaks with maxima at 3.77 nm and 4.62 nm, i.e., separated by 0.85 nm and widths (full width at half maximum - fwhm) of 0.37 nm and 0.39 nm, respectively. The peak at 3.77 nm has a shoulder at shorter distances indicating a third distance component.

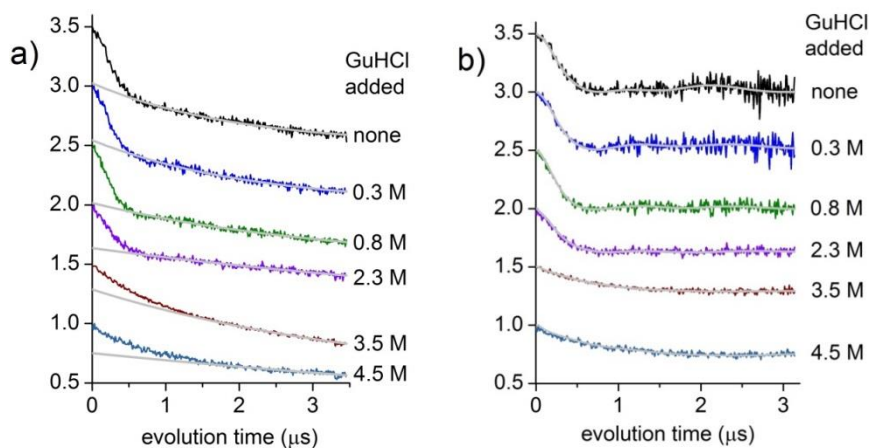


Figure 5.3 The DEER traces for fdx-SL measured at different concentrations of GuHCl. a) The traces obtained from the DEER measurements are shown with their optimal background fit (in grey). Individual traces are normalized and shifted vertically for better viewing. b) The traces obtained after division by the background fit. In b) the fitted traces (in grey) correspond to distance distributions ($\alpha = 100$) that are shown in Figure 5.4 and 5.5b.

The measured distances are between the nitroxide groups of the two spin labels. Each nitroxide group is separated from the protein backbone by the spin-label linker, which has a length of about 0.5 nm. Therefore, the spin-label linker has to be taken into account to relate the distance measured by DEER to the protein structure. Spin-label-linker conformations were calculated by the rotamer-library based method MMM^[18] with the X-ray structure of holo-fdx as input (PDB entry 1YOB^[19]). The X-ray structure of fdx contains two proteins in the asymmetric unit of the crystal (monomer A and monomer B). The distance distributions calculated for the two proteins in the asymmetric unit are shown in Figure 5.4. The MMM distance distributions of both monomers, A and B, each have two peaks, which are separated by 0.38 nm (monomer A) and 0.40 nm (monomer B). The two peaks derive from two families of linker conformations, since, in the X-ray structure, the protein backbone has a unique conformation. In Figure 5.1 selected locations of the nitroxide are shown as spheres. Particularly, the spin label at position 69 has only few accessible conformations, whereas the spin label at 131 has an extensive cloud of nitroxide positions, suggesting that the two families derive from two sets of conformations of the spin label at position 69. The centres of the distributions of monomer A and B differ by 0.15 nm. Figure 5.4 further shows that the distributions derived from the X-ray structure are centred at shorter distances than those obtained from the DEER measurement at 0.3 M GuHCl. The distance distribution at 0.3 M GuHCl (Figure 5.5), differs from that of fdx-SL in the absence of GuHCl (Figure 5.4), although for both samples the protein should still be fully folded^[8].

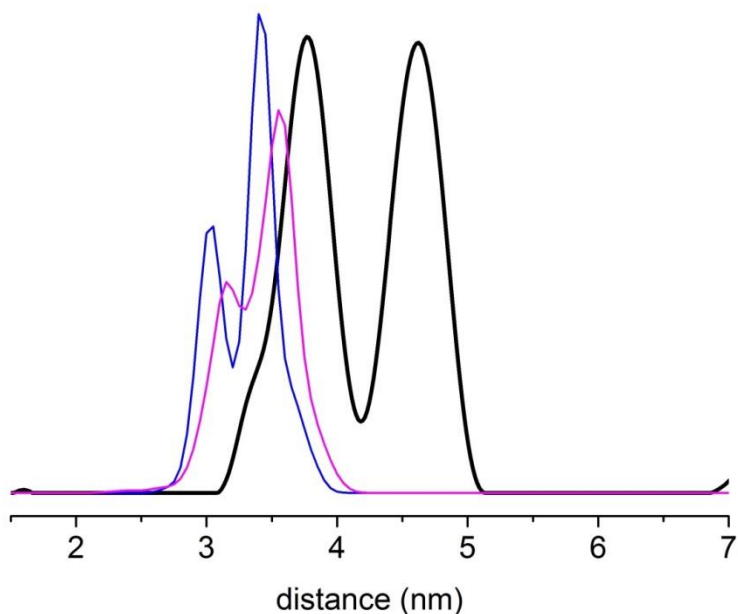


Figure 5.4 Distance distribution of native fdx-SL with regularization parameter 100 (black) and those derived by simulation with MMM from the crystal structure of fdx (blue, purple). Crystal structure: PDB entry 1YOB, using monomers A and B in the crystallographic unit cell.

Figure 5.5a and b show distance distributions obtained at different GuHCl concentrations. Data from two regularization parameters^[20] are shown: a) appropriate for the distributions at GuHCl concentrations ≤ 2.3 M and b) for > 2.3 M. To monitor the unfolding we use the distance distribution of 0.3 M GuHCl as a reference. With respect to the modulation depth (Figure 5.3b), the DEER data fall into two regimes: from 0.3 M to 2.3 M GuHCl, the modulation depth accounts for $> 94\%$ of the protein population. From 2.3 to 3.5 M GuHCl the protein population that contributes to the distance distribution halves (Table 5.1), showing that at 3.5 M GuHCl a large fraction of the protein is in conformations where the spin-spin distance of the two nitroxides is outside the measurement range of the DEER experiment, i.e., smaller than 2 nm and/or

larger than 6 nm. Given the low modulation depth, and the smooth decay of the DEER time trace, the exact shape of the distance distribution is less certain than the distribution for the lower GuHCl concentrations. A higher regularization parameter, i.e., $\alpha = 100$ has to be used to describe the distributions at 3.5 and 4.5 M properly, as will be discussed below.

Table 5.1 Overall parameters of the DEER derived distance distributions upon fdx unfolding. Parameters are derived from the distributions with regularization parameter 100.

| concentration GuHCl (M) | coupled spins (%) ^a | mean distance $\langle r \rangle$ (nm) | standard deviation σ (nm) |
|----------------------------|-----------------------------------|--|--|
| 0.3 | 109 | 4.08 | 0.45 |
| 0.8 | 117 | 4.01 | 0.51 |
| 2.3 | 94 | 4.25 | 0.58 |
| 3.5 | 40 | 5.3 | 1.55 |
| 4.5 | 48 | 5.38 | 1.62 |

^a Calculated from the number of spins: 2 = 100%, 1 = 0%. The number of spins yielded by DeerAnalysis has an overall error of about 5%, corresponding to an error of 10% in the percentage of coupled spins (see reference [21]).

To describe the distance distributions in Figure 5.5a, Gaussian bands are fitted to the most intense peaks (Figure 5.5c). Several smaller, less intense peaks, marked by an asterisk, were shown not to be significant by the suppression tool in DEER analysis, meaning that their contribution to the DEER time-trace does not cause a significant deviation, given the noise of the curve. The distributions at 0.3 M and 0.8 M GuHCl are well described by three Gaussians (labelled $N_1 - N_3$ in Table 5.2) with slightly different parameters for these two GuHCl concentrations. As an illustration, from 0.3 to 0.8 M GuHCl, the peak N_1 shifts by 0.16 nm to lower distances and all widths increase; the largest increase in

width is observed for the peak N_3 , which increases by 0.09 nm. The distribution at 2.3 M GuHCl requires five Gaussians. Three of them ($N_1 - N_3$) are similar to those observed at lower GuHCl concentrations. A new peak appears at 3 nm (MG_1) and a shoulder at peak N_2 shows an underlying additional peak (MG_2). The area under the MG_1 and MG_2 peaks accounts for in total 17% of the five Gaussians in the distribution.

Table 5.2 Parameters of the Gaussian fits of DEER distance distributions. X_c : centre of Gaussian, W: full width at half maximum, A: area under the curve at 0.3 M, 0.8 M, and 2.3 M GuHCl, regularization parameter 10.

| peaks | | GuHCl concentration | | | |
|--------|------------|---------------------|-------|-------|-------|
| | | 0 | 0.3 M | 0.8 M | 2.3 M |
| N_1 | X_c (nm) | 3.32 | 3.58 | 3.42 | 3.48 |
| | W (nm) | 0.13 | 0.22 | 0.23 | 0.16 |
| | A | 7% | 22% | 20% | 9% |
| N_2 | X_c (nm) | 3.78 | 3.98 | 3.91 | 3.95 |
| | W (nm) | 0.28 | 0.27 | 0.35 | 0.38 |
| | A | 43% | 49% | 58% | 49% |
| N_3 | X_c (nm) | 4.62 | 4.69 | 4.68 | 4.85 |
| | W (nm) | 0.36 | 0.27 | 0.36 | 0.55 |
| | A | 50% | 29% | 22% | 25% |
| MG_1 | X_c (nm) | N.A. | N.A. | N.A. | 3.05 |
| | W (nm) | | | | 0.15 |
| | A | | | | 9% |
| MG_2 | X_c (nm) | N.A. | N.A. | N.A. | 4.29 |
| | W (nm) | | | | 0.23 |
| | A | | | | 8% |

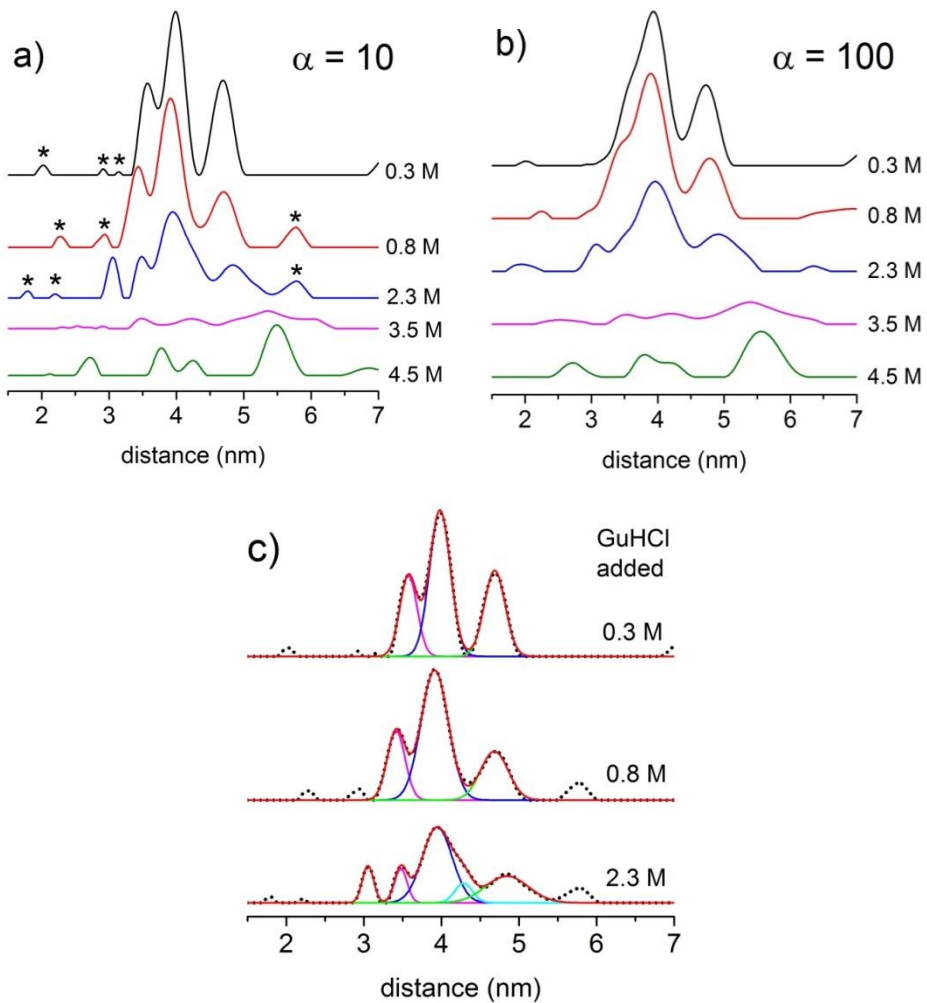


Figure 5.5 Effect of GuHCl concentration on distance distributions of fdx-SL. The distance distributions were obtained with the regularization parameter of a) $\alpha = 10$ and b) $\alpha = 100$, and c) fits of Gaussians to the top three distance distributions in a).

The mean distance of the distribution $\langle r \rangle$ and the width, given as the standard deviation σ , reveal the overall features of the distance distributions for all GuHCl concentrations (Table 5.1). The mean distance remains almost constant between 0.3 and 2.3 M GuHCl and increases by 1 nm at 3.5 and 4.5 M GuHCl, with concomitant tripling of the standard deviation. Figure 5.6 is a graphical representation of the data in Table 5.1.

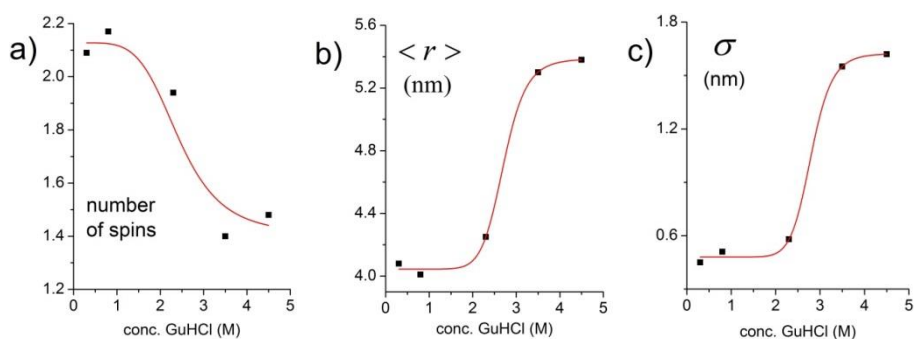


Figure 5.6 Representations of the unfolding of fdx-SL as a function of the concentration of GuHCl through three observables derived from the EPR experiments: a) the number of spins, b) the mean distance $\langle r \rangle$ for $\alpha = 100$, and c) the standard deviation σ for $\alpha = 100$. The red lines merely serve as a guide to the eye. The figures are graphical representations of the data in Table 5.1.

5.4 Discussion

We have investigated the unfolding of fdx in the presence of different amounts of the unfolding agent GuHCl. Before describing the changes in protein structure under the influence of the unfolding agent, the distance distribution of the native fdx is discussed in terms of what is known about the structure of fdx in the folded state.

The native state of holo-fdx

In the folded, native state, fdx is a globular protein with a well-defined, single structure. Nevertheless, there are two peaks in the distance distribution of the native protein (Figure 5.4), the widths of which are typical of the intrinsic flexibility of the spin-label side chain attached to a well-structured protein^[22]. Modelling the spin-label side-chain conformation with MMM also yields two-peaked distance distributions, albeit at shorter distances than observed experimentally, showing that the two distances observed in the measured distance distribution stem from two families of spin-label linker conformations. The overall longer distances measured could derive from a more extended conformation of the loop between residues 126 to 148, which contains one of the spin-label sites, residue 131. Changes in the conformation of the loop will affect the mutual distance between the spin labels at position 131 and 69. The second factor is the protein structure around the cysteine at position 69. In the native protein, the cysteine at this position points to the interior of the protein. In the spin-labelled state, this cysteine is more likely to switch to a conformation that projects the spin-label side chain to the exterior of the protein, thereby increasing the distance between the nitroxides of the two spin labels. Such a change in the side-chain and backbone conformation is not accounted for in MMM, explaining the difference between the MMM and the DEER-derived distances of the native protein. The distance distribution

observed by DEER, therefore, is compatible with what is known about the native structure of fdx. At a GuHCl concentration of 0.3 M, the protein is in the fully folded state^[8], however, the distance and distance distribution differs slightly from that of fdx in the absence of GuHCl: The peak at 3.8 nm splits into two, leading to a three-peaked distance distribution described by the Gaussian peaks $N_1 - N_3$. We attribute these changes to a local influence of GuHCl on the spin-label conformation.

Unfolding of fdx followed by DEER

Similarly to previous EPR studies on other proteins^[1;3], also for fdx we find systematic changes of the EPR parameters with respect to the GuHCl concentration, showing that DEER provides a method to follow protein unfolding. To analyse the changes in detail, we use the distance distribution of 0.3 M GuHCl as a reference to ensure that the effects of GuHCl derive from the unfolding of the protein and not from a local influence of GuHCl on the spin-label conformation.

According to the DEER results, the most remarkable change in the structure of fdx during unfolding occurs between 2.3 and 3.5 M GuHCl. Up to a concentration of 2.3 M GuHCl, the distance distributions account for almost the entire protein population and the shape of the distance distribution is that of a structured protein. At 3.5 and 4.5 M GuHCl, the distance distributions become broader and the average distance $\langle r \rangle$ becomes larger with increasing GuHCl concentrations (Table 5.1). A larger fraction of fdx-SL has distances that are outside the DEER observation window, i.e., below 2 nm or above 6.5 nm. Distances below 2 nm can be excluded, because they would give rise to a dipolar broadening in the frozen solution cw EPR spectra, which does not occur (see Results). In summary, the protein goes from a state with a limited number of conformations and a relative compact structure at lower GuHCl

concentrations to a large number of conformations and a more extended state at GuHCl concentrations of 3.5 M and above, in keeping with a largely unfolded state. In the following we take a closer look at the lower GuHCl concentrations.

At concentrations of 2.3 M GuHCl and below, the protein has all characteristics of a structured protein. To interpret the results at these lower GuHCl concentrations, we take the three-peak distance distribution ($N_1 - N_3$, Table 5.2) in Figure 5.5a, 0.3 M GuHCl, as the signature of natively folded protein. Thus, at 0.8 M GuHCl, the protein is predominantly in the native conformation. There are small differences between the parameters of $N_1 - N_3$ at 0.3 and 0.8 M GuHCl, which we interpret as changes in the local spin-label environment by GuHCl (Table 5.2).

At 2.3 M GuHCl, additional distance peaks (MG_1 and MG_2 , Figure 5.5a and c, Table 5.2) appear. The widths of these peaks are in the order of the widths of the native state peaks, showing that in the corresponding state the protein has a well-defined structure. To estimate the populations of the different states of the protein at 2.3 M GuHCl, not only the relative contribution of the distance peaks MG_1 and MG_2 to the remaining peaks $N_1 - N_3$, but also the 15% of protein with distances outside the DEER range are taken into account. Total populations of 72% native, 14% folding intermediate, and 15% unfolded protein result. In this interpretation we count the entire population under the peaks $N_1 - N_3$ as native protein, however, this need not be. The relative intensities of the peaks N_1 , N_2 and N_3 at 2.3 M GuHCl are not identical to those at lower GuHCl concentrations. The deviation is largest for N_1 , which has an intensity that is 11% smaller than in the native protein (0.3 M GuHCl). A folding intermediate that accidentally has a distance similar to one of the native ones, or, perhaps more likely, an underlying broader distance distribution, could change the apparent relative intensities of the peaks $N_1 - N_3$. We, therefore, consider the native state population of 72% as an upper limit.

Counting, somewhat arbitrarily, the entire loss of intensity at N_1 as population of folding intermediate would result in 61% native and 25% folding intermediate, which we estimate to be lower limits of native-state population, and upper limits of folding-intermediate population, respectively.

Therefore, we postulate that between 14% and 25% of the protein at 2.3 M GuHCl are in a folding-intermediate state, characterized by distance contributions MG_1 and MG_2 . Given that the MG_1 and MG_2 distances differ by 1.24 nm, MG_1 and MG_2 presumably reflect proteins in different conformations, rather than a single backbone conformation with different families of nitroxide side-chain orientations. Consequently, a certain population of the protein attains a fold, in which residues 69 and 131 are closer to each other than in the native state (MG_1), and one in which the distance is intermediate amongst the distances seen in the native state (MG_2).

The presence of a folding intermediate was also suggested by recent single-molecule Förster resonance energy-transfer (FRET) experiments, which targeted the distance between the same two positions^[23]. Below about 1.5 M GuHCl, this intermediate has a shorter inter-dye distance than the native protein. At higher GuHCl concentrations, this intermediate gradually unfolds into a less well-structured state, characterized by longer distances than in the native protein. The coexistence of the intermediate with the native-like protein seemed to occur at overall lower GuHCl concentrations than in the present EPR study. This is reasonable, given that in the optical study apo-fdx was investigated, which has a lower stability and therefore unfolds at lower GuHCl concentrations than the holo-fdx we study here. Furthermore, differences are to be expected because the labels are different. For EPR nitroxide spin labels are used, whereas the labels used in the FRET-experiments are more bulky and could additionally destabilize the folding intermediate. Further differences

could arise from the different intervals between the GuHCl concentrations in both studies.

We show that by DEER local structure in the unfolding protein can be measured and present evidence for a folding intermediate that is locally more compact than the native state and is in coexistence with a folding intermediate that has a distance between residues 69 and 131 that is similar to the native state. The DEER method provides distance distributions. Their widths give information about the degree of structure of a particular state and thereby enable us to discriminate between unfolded states and folding intermediates.

References

- [1] D.I. Kreimer, R. Szosenfogel, D. Goldfarb, I. Silman, L. Weiner, 2-State Transition Between Molten Globule and Unfolded States of Acetylcholinesterase As Monitored by Electron-Paramagnetic-Resonance Spectroscopy. *Proceedings of the National Academy of Sciences of the United States of America* **91** (1994) 12145-12149.
- [2] W.L. Hubbell, H.S. Mchaourab, C. Altenbach, M.A. Lietzow, Watching proteins move using site-directed spin labeling. *Structure* **4** (1996) 779-783.
- [3] K. Deweerdt, V. Grigoryants, Y.H. Sun, J.S. Fetrow, C.P. Scholes, EPR-detected folding kinetics of externally located cysteine-directed spin-labeled mutants of iso-1-cytochrome c. *Biochemistry* **40** (2001) 15846-15855.
- [4] V.M. Grigoryants, K.A. DeWeerd, C.P. Scholes, Method of rapid mix EPR applied to the folding of bi-spin-labeled protein as a probe for the dynamic onset of interaction between sequentially distant side chains. *Journal of Physical Chemistry B* **108** (2004) 9463-9468.
- [5] V.M. Grigoryants, A.V. Veselov, C.P. Scholes, Variable velocity liquid flow EPR applied to submillisecond protein folding. *Biophysical Journal* **78** (2000) 2702-2708.
- [6] K.B. Qu, J.L. Vaughn, A. Sienkiewicz, C.P. Scholes, J.S. Fetrow, Kinetics and motional dynamics of spin-labeled yeast iso-1-cytochrome c .1. Stopped-flow electron paramagnetic resonance as a probe for protein folding/unfolding of the C-terminal helix spin-labeled at cysteine 102. *Biochemistry* **36** (1997) 2884-2897.
- [7] A. Sienkiewicz, A.M.D. Ferreira, B. Danner, C.P. Scholes, Dielectric resonator-based flow and stopped-flow EPR with rapid field scanning: A methodology for increasing kinetic information. *Journal of Magnetic Resonance* **136** (1999) 137-142.
- [8] S. Lindhoud, A.H. Westphal, J.W. Borst, C.P.M. van Mierlo, Illuminating the Off-Pathway Nature of the Molten Globule Folding Intermediate of an alpha-beta Parallel Protein. *Plos One* **7** (2012) 1-10.
- [9] Y.J.M. Bollen, S.M. Nabuurs, W.J.H. van Berkel, C.P.M. van Mierlo, Last in, first out. *Journal of Biological Chemistry* **280** (2005) 7836-7844.
- [10] S.M. Nabuurs, B.J. de Kort, A.H. Westphal, C.P.M. van Mierlo, Non-native hydrophobic interactions detected in unfolded apoflavodoxin by paramagnetic relaxation enhancement. *European Biophysics Journal with Biophysics Letters* **39** (2010) 689-698.
- [11] S.M. Nabuurs, C.P.M. van Mierlo, Interrupted Hydrogen/Deuterium Exchange Reveals the Stable Core of the Remarkably Helical Molten Globule of alpha-beta Parallel Protein Flavodoxin. *Journal of Biological Chemistry* **285** (2010) 4165-4172.
- [12] S.M. Nabuurs, A.H. Westphal, M. aan den Toorn, S. Lindhoud, C.P.M. van Mierlo, Topological Switching between an alpha-beta Parallel Protein and a Remarkably Helical Molten Globule. *Journal of the American Chemical Society* **131** (2009) 8290-8295.
- [13] S.M. Nabuurs, A.H. Westphal, C.P.M. van Mierlo, Noncooperative Formation of the Off-Pathway Molten Globule during Folding of the alpha-beta Parallel Protein Apoflavodoxin. *Journal of the American Chemical Society* **131** (2009) 2739-2746.

- [14] S.M. Nabuurs, A.H. Westphal, C.P.M. van Mierlo, Extensive Formation of Off-Pathway Species during Folding of an alpha-beta Parallel Protein Is Due to Docking of (Non)native Structure Elements in Unfolded Molecules. *Journal of the American Chemical Society* **130** (2008) 16914-16920.
- [15] B.A. Shirley, Urea and Guanidine Hydrochloride Denaturation Curves. *Protein Stability and Folding: Theory and Practice*, Humana Press, New Jersey, 1995, pp. 177-190.
- [16] G. Jeschke, Determination of the nanostructure of polymer materials by electron paramagnetic resonance spectroscopy. *Macromolecular Rapid Communications* **23** (2002) 227-246.
- [17] G. Jeschke, V. Chechik, P. Ionita, A. Godt, H. Zimmermann, J. Banham, C.R. Timmel, D. Hilger, H. Jung, DeerAnalysis2006 - a comprehensive software package for analyzing pulsed ELDOR data. *Applied Magnetic Resonance* **30** (2006) 473-498.
- [18] Y. Polyhach, E. Bordignon, G. Jeschke, Rotamer libraries of spin labelled cysteines for protein studies. *Physical Chemistry Chemical Physics* **13** (2011) 2356-2366.
- [19] S. Alagaratnam, G. Van Pouderoyen, T. Pijning, B.W. Dijkstra, D. Cavazzini, G.L. Rossi, W.M.A.M. Van Dongen, C.P.M. van Mierlo, W.J.H. van Berkel, G.W. Canters, A crystallographic study of Cys69Ala flavodoxin II from *Azotobacter vinelandii*: Structural determinants of redox potential. *Protein Science* **14** (2005) 2284-2295.
- [20] G. Jeschke, A. Koch, U. Jonas, A. Godt, Direct conversion of EPR dipolar time evolution data to distance distributions. *Journal of Magnetic Resonance* **155** (2002) 72-82.
- [21] B.E. Bode, D. Margraf, J. Plackmeyer, G. Durner, T.F. Prisner, O. Schiemann, Counting the monomers in nanometer-sized oligomers by pulsed electron - electron double resonance. *Journal of the American Chemical Society* **129** (2007) 6736-6745.
- [22] M.G. Finiguerra, M. Prudencio, M. Ubbink, M. Huber, Accurate long-range distance measurements in a doubly spin-labeled protein by a four-pulse, double electron-electron resonance method. *Magnetic Resonance in Chemistry* **46** (2008) 1096-1101.
- [23] S. Lindhoud *et al.*, data to be published.